Soil organic phosphorus transformations along a coastal dune chronosequence under New Zealand temperate rain forest

Benjamin L. Turner, Andrew Wells & Leo M. Condron

Biogeochemistry
An International Journal

ISSN 0168-2563
Volume 121
Number 3

Biogeochemistry (2014) 121:595-611
DOI 10.1007/s10533-014-0025-8

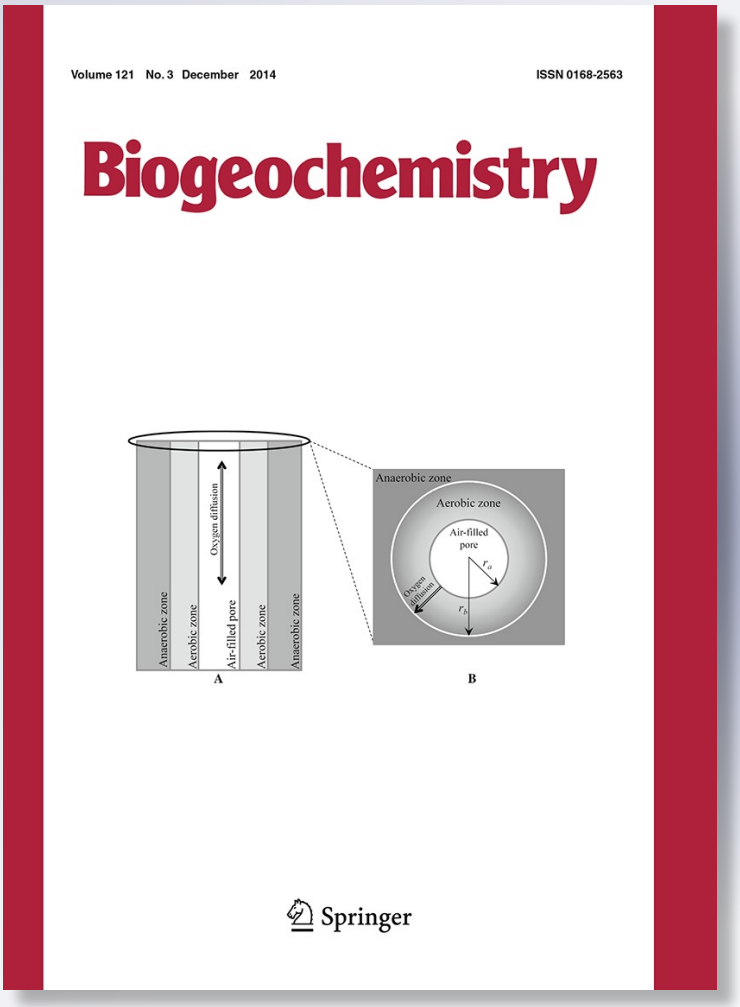

Springer

Biogeochemistry (2014) 121:595–611
DOI 10.1007/s10533-014-0025-8

Soil organic phosphorus transformations along a coastal dune chronosequence under New Zealand temperate rain forest

Benjamin L. Turner · Andrew Wells · Leo M. Condron

Received: 17 February 2014 / Accepted: 9 August 2014 / Published online: 28 August 2014

Abstract The chemical composition of soil phosphorus can vary markedly during pedogenesis, which has implications for phosphorus availability to plant and microbial communities during long-term ecosystem development. We used NaOH–EDTA extraction and solution ^{31}P NMR spectroscopy to examine changes in soil phosphorus composition along the Haast chronosequence, a 6,500 year sequence of coastal dunes under lowland temperate rain forest on the west coast of the South Island of New Zealand. Soils along the chronosequence contained a variety of inorganic (orthophosphate, pyrophosphate, and long-chain polyphosphate) and organic (phosphomonoesters, phosphodiesters, and phosphonates) phosphorus compounds, although long-chain polyphosphates were detected only in the organic horizon and phosphonates were detected only in mineral soil. The concentrations of most compounds increased initially during the first few hundred years of pedogenesis and then declined as soils aged. However, concentrations of phospholipids, DNA, and long-chain polyphosphate all increased markedly in the organic horizon of older sites. The four inositol hexakisphosphate stereoisomers (*myo*, *scyllo*, *neo*, and D-*chiro*) accounted for a considerable proportion of the phosphomonoesters in mineral soil along the sequence (36–52 % of the organic phosphorus), but were not detected in quantifiable concentrations in the youngest mineral soil and all but one organic horizon. Concentrations of the two most abundant isomers (*myo*- and *scyllo*) declined along the chronosequence, but the *scyllo* isomer increased markedly as a proportion of the soil organic phosphorus as soils aged. Amorphous aluminum and iron oxides (i.e., extractable in acid-ammonium oxalate) increased continually throughout the chronosequence, indicating that the decline in inositol hexakisphosphate is due to low phosphorus availability rather than a decline in stabilization potential. Overall, these results provide further evidence that the chemical composition of organic and inorganic phosphorus pools vary markedly during pedogenesis, which has important implications for our understanding of biologically-available organic phosphorus during ecosystem development.

Keywords Haast chronosequence · Phosphomonoesters · Phosphodiesters · DNA · Inositol phosphate · Phytate · *scyllo*-Inositol hexakisphosphate · *neo*-Inositol hexakisphosphate · D-*chiro*-Inositol hexakisphosphate · Polyphosphate · Solution ^{31}P NMR spectroscopy

Responsible Editor: Stephen Porder.

B. L. Turner (✉)
Smithsonian Tropical Research Institute,
Apartado 0843-03092, Balboa, Ancon, Republic of Panama
e-mail: turnerbl@si.edu

A. Wells · L. M. Condron
Agriculture and Life Sciences, Lincoln University,
Lincoln, PO Box 85084, 7647 Christchurch, New Zealand

Introduction

Soil phosphorus (P) transformations during pedogenesis determine patterns of nutrient availability and limitation, which in turn shape plant and microbial communities during long-term ecosystem development (Walker and Syers 1976; Vitousek 2004; Peltzer et al. 2010). Total P declines rapidly in young soils as P is lost in runoff at a greater rate than it is replenished by bedrock weathering and inputs from the atmosphere. At the same time, there are changes in the chemical nature of the P remaining in the soil: most of the P in young soils is in primary minerals (e.g., apatite), but this is converted during the early stages of pedogenesis into organic compounds and inorganic phosphates associated with secondary minerals such as amorphous iron and aluminum oxides. Eventually, over long timescales, soil P is depleted to low concentrations and consists almost entirely of organic or occluded inorganic P.

The changes in soil P composition during pedogenesis mean that plants and microbes must increasingly obtain the majority of their P from the recycling of organic P as ecosystem development proceeds. Soil organic P is not a homogenous pool, but includes a variety of compounds that differ markedly in their stability and biological availability in the soil environment (Condron et al. 2005). For example, most soils contain a mixture of phosphomonoesters such as inositol hexakisphosphate (IP_6) and mononucleotides, and phosphodiesters such as nucleic acids and phospholipids. In general, phosphodiesters are weakly sorbed in soils and turn over more rapidly than compounds such as the inositol phosphates, which can be stabilized by strong associations with metal oxides (Bowman and Cole 1978; Condron et al. 2005; Celi and Barberis 2007). Soils also contain phosphonates, which have a direct C–P bond, as well as organic polyphosphates such as adenosine triphosphate. In addition, soils can contain inorganic polyphosphates, which can be considered functionally similar to the phosphomonoesters due to their hydrolysis by phosphomonoesterase enzymes.

Recent evidence indicates that the composition of the soil organic P can undergo marked changes during long-term pedogenesis (McDowell et al. 2007; Turner et al. 2007; Vincent et al. 2013). This has important implications for understanding patterns in plant and microbial communities during ecosystem development, because organisms vary in the extent to which they are adapted to acquire P from the various forms in soil (Hill and Richardson 2007; Turner 2008a). Long-term changes in the chemical composition of soil P might therefore influence the presence or performance of plants or microbes during ecosystem development.

We previously reported that along the Franz Josef chronosequence, on the west coast of the South Island of New Zealand, DNA increased and IP_6 declined as a proportion of the organic P as soils aged over 120,000 years (Turner et al. 2007). This was surprising, because phosphodiesters such as DNA are typically considered to be relatively labile in soils, whereas the inositol phosphates are considered to be a stable fraction of the soil organic P (Condron et al. 2005; Celi and Barberis 2007). Similar results were reported for other New Zealand chronosequences on sand, basalt, and alluvium (McDowell et al. 2007), but not for a 7,800 year sequence of marine uplift terraces in Sweden in which inositol phosphate concentrations were low, presumably because only the organic horizon was studied (Vincent et al. 2013).

The accumulation of DNA and pyrophosphate could be due to the incorporation of these compounds into recalcitrant soil organic matter (Turner et al. 2007), or the increasing quantitative importance of the soil microbial biomass as soils age (Turner et al. 2013; Vincent et al. 2013). The decline in IP_6 in old soils could reflect a decline in P availability in older soils, or a decline in amorphous metal oxides, which provide reactive surfaces that stabilize inositol phosphates. Amorphous Al and Fe follow a predictable pattern during soil development, increasing initially in the early stages of pedogenesis, and then declining in strongly weathered soils as the amorphous compounds 'ripen' into crystalline forms (Chadwick and Chorover 2001). It was not possible to isolate the causative factor in the decline in IP_6 along the Franz Josef chronosequence, because P availability and amorphous metal oxides both declined in old soils. Information on additional chronosequences is therefore required to address these hypotheses and determine whether the patterns in soil organic P compounds during long-term pedogenesis apply to ecosystems more broadly.

We have recently studied a chronosequence of soils formed on coastal sand dunes at Haast, New Zealand. The Haast chronosequence approximates an ideal chronosequence, because topography, parent material,

and dune ages are well-constrained, and the site supports undisturbed temperate rain forest that has been present in the region throughout the lifespan of the chronosequence. The soils develop into Spodosols within a few thousand years, involving the rapid depletion of primary mineral P and accumulation of organic P within the first few hundred years of ecosystem development (Turner et al. 2012b). Forest biomass peaks after a few hundred years and then declines, and there are marked changes in the composition of the tree community, from dominance by conifers in the Podocarpaceae on young soils, to a mixed conifer–angiosperm forest on old soils, including the ectomycorrhizal species *Nothofagus menziesii* on the oldest dunes (Turner et al. 2012c). There are also shifts in the soil bacterial community along the sequence, with declines in the abundance of Actinobacteria, Bacteroidetes, Betaproteobacteria, and Firmicutes, but increases in Acidobacteria, Alphaproteobacteria, and Planctomycetes, as soils age over 6,500 years (Jangid et al. 2013). Overall, we assume that P becomes increasingly limiting to ecosystem processes in the late stages of the chronosequence based on a number of lines of evidence, including declining available and total P concentrations, widening N:P ratios in soils and plant tissue, and a marked decline in tree basal area on old soils, consistent with the concept of forest retrogression (Turner et al. 2012b, c; Eger et al. 2013).

The marked decline in total P and high proportion of organic P ($\sim$80 % of the total P in mineral soil for the majority of the sequence) along the Haast chronosequence offers an important opportunity to examine changes in the composition of the soil organic P, because amorphous metal oxides increase continually along the chronosequence, while P availability declines markedly on old soils (Turner et al. 2012b). Our aims were: (1) to assess changes in the composition of P in mineral soil and the organic horizon busing NaOH–EDTA extraction and solution ^{31}P NMR spectroscopy, and (2) determine the extent to which P compounds might be influenced by declining P availability or mineralogical changes in metal oxides.

Methods

The Haast chronosequence

The Haast dune system is located northeast of the town of Haast, on the west coast of the South Island of New Zealand (approximate center of the sequence 43°49′22″ S, 169°04′43″ E). The system extends approximately 10 km alongshore and 5 km inland, with dunes running parallel to the coastline and rising up to 20 m above adjacent dune slacks. Dune formation is initiated by earthquakes along the Alpine Fault, which cause widespread land disturbance (Wells and Goff 2007). After each earthquake, a pulse of sediment is transported rapidly to the ocean via the Haast River and is then deposited along the coastline by long-shore drift to form a dune. Dune building has occurred following all known earthquakes since A.D. 1200 and dunes appear to have been forming since sea level stabilized ca. 6,500 years ago (Wells and Goff 2006).

Dates of dune formation were obtained from historical records, tree rings, and a ^{14}C date (Table 1). Parent material originates in the Southern Alps and is predominantly well-foliated schist masses, including semi-schistose greywacke and argillite. The particle size distribution (Turner et al. 2012b) and mineralogy (Palmer et al. 1986) of the unweathered parent sand is similar across the chronosequence, and consists of 40–50 % quartz, with the remainder feldspar, mica and chlorite. Soil P in the youngest dune is almost all primary mineral phosphate (Turner et al. 2012b), suggesting that there the parent material undergoes only very limited weathering prior to dune deposition. All the dunes are linear and continuous features running parallel with the coastline, although they vary in height, presumably due to the magnitude of the earthquake events and the loose material they generated. Erosion is assumed to be of minor importance given the absence of surface runoff due to the sandy nature of the soil.

Mean annual rainfall between 1941 and 1976 at Haast Beach, approximately 15 km from the chronosequence, was 3,455 mm. Rainfall ($\geq$1 mm) occurs on 178 days per year and no month receiving $<$200 mm. Mean annual temperature is 11.3 °C, with mean monthly values between 14.9 °C in February to 7.4 °C in July. Climate at the site has probably varied considerably since the onset of dune formation, although the region has been under mixed conifer–broadleaved rain forest since 7700 B.P., and probably since 11,400 B.P. (Li et al. 2008). The conifers are dominated by members of the Podocarpaceae, although the dominant podocarp species, as well as woody angiosperms and tree ferns, varies along the sequence (Turner et al. 2012c). Early dunes up to

Table 1 Ages and soil properties of ten dune stages along the Haast dune sequence, New Zealand (Turner et al. 2012b)

Dune stage	Dune age[a] (years B.P.)	Soil taxonomy	Organic horizon					Mineral soil (0–20 cm)					
			Depth (cm)	pH	C (%)	N (%)	P (mg P kg^{-1})	pH	C (%)	N (%)	P (mg P kg^{-1})	Al_{ox} (mmol kg^{-1})	Fe_{ox} (mmol kg^{-1})
1	181	Typic Udipsamment	<1	5.6	22.93	1.10	885	4.7	0.91	0.07	311	6.3	10.5
2	290	Typic Udipsamment	5	4.1	37.57	0.96	691	4.2	2.99	0.17	194	24.3	38.0
3	392	Typic Udipsamment	6	5.0	32.46	1.03	706	4.2	3.13	0.16	229	28.0	44.9
4	517	Typic Udipsamment	3	4.7	36.05	0.99	654	4.1	3.17	0.17	211	31.2	47.2
6	787	Typic Udipsamment	4	5.6	25.42	0.82	646	4.1	3.28	0.19	248	20.2	29.7
8	1,826	Spodic Udipsamment	21	3.7	50.01	1.60	622	3.9	1.87	0.09	155	50.7	52.9
11	3,384	Spodic Udipsamment	25	3.9	47.77	1.52	599	3.9	2.04	0.09	142	62.6	90.0
12	3,903	Typic Placorthod	22	3.8	48.81	1.44	485	3.8	2.09	0.09	105	56.8	61.2
13	4,422	Typic Placorthod	28	4.1	46.13	1.38	492	3.7	2.52	0.11	111	67.6	70.5
17	6,500	Typic Placorthod	17	3.8	50.88	1.44	611	3.6	2.33	0.10	102	88.6	107.6

Values are means of three replicate plots per dune, each of which was a composite of ten individual cores. The Typic Udipsamments had no eluvial or placic horizons, Spodic Udipsamments had an eluvial horizon but no placic horizon, and Typic Placorthods had both eluvial and placic horizons

Al_{ox} oxalate-extractable (amorphous) aluminum, Fe_{ox} oxalate-extractable (amorphous) iron

[a] Dates are from the year of sampling (2007); stages 1–6 were dated by tree rings (Wells and Goff 2007), stage 17 by a radiocarbon date, and stages 8–13 were estimated by assuming an equal number of years between dune stages 6 and 17 (Turner et al. 2012b)

about 500 years old are dominated by *Dacrydium cupressinum* (Podocarpaceae) and tree ferns (*Dicksonia squarrosa*, *Cyathea smithii*). Older dunes support abundant *Weinmannia racemosa* (Cunoniaceae) and the dominant podocarp is *Prumnopitys ferruginea*. On the oldest dune, *N. menziesii*, an ectomycorrhizal tree, is also present (27 % of basal area of stems ≥10 cm diameter at breast height) (Turner et al. 2012c).

Summary of changes in soil properties along the Haast sequence

Soils along the Haast chronosequence develop rapidly to Spodosols (podzols) under the perhumid climate (Turner et al. 2012b). Soils on young dunes (<800 years B.P.) are Typic Udipsamments (Entisols), while soils on Intermediate-aged dunes are Spodic Udipsamments (Entisols), with a thick organic horizon and a well-developed albic (eluvial) horizon, but no placic horizon or spodic B horizon. Soils on older dunes (3,900–6,500 years B.P.) are Typic Placorthods (Spodosols), characterized by a thick organic horizon, a bleached albic horizon, a spodic horizon (i.e., subsoil accumulation of iron and organic matter), and a cemented iron pan (placic horizon). The thickness of the organic horizon increases from <1 cm on the youngest dune to 17–28 cm on the older dunes and there is rapid acidification and depletion of exchangeable base cations in the early stages of pedogenesis. Soils are very acidic, with mineral soil pH (measured in water) ≤4.2 for the majority of the sequence, declining to ~3.5 on the oldest dunes (Turner et al. 2012b). Topsoil texture (upper mineral soil) is sand or loamy sand throughout.

Total P concentrations in both organic and surface mineral soil horizons decline rapidly in the first few hundred years of pedogenesis, from high initial values in young soils to the lowest values in old soils (Table 1). The decline in total P in mineral soil is accounted for mainly by the disappearance of primary mineral P (i.e., acid-extractable inorganic phosphate) within the first few hundred years. Organic P (determined by the ignition procedure; Saunders and Williams 1955) accounted for 72–84% of the total P for all but the youngest dune (~20 %) (Turner et al. 2012b). In contrast, total carbon and nitrogen concentrations increase from low values in the young soils to maximum values in older soils, with a slight decline in the total nitrogen concentration at the oldest sites (Table 1). The corresponding N:P ratios increase with soil age, indicative of increasing P limitation. Soil physical and chemical properties were reported previously (Turner et al. 2012b), but in addition we determined amorphous metal oxides in mineral soils from the plots by extraction in acid-ammonium oxalate (Loeppert and Inskeep 1996) (see below).

Soil sampling and extraction

Soils from ten dunes were studied (Table 1). Nine of these were within the main dune system to the northeast of the Haast River, while one (Dune Unit 6, 1220 A.D.) was southwest of the river. Dunes were described in detail previously (Turner et al. 2012b). In February 2007 we sampled surface soils from three replicate 10 × 20 m plots located along the dune crest at each site. Plots were located from the dune crest to the upper back-slope (the area of dune most likely to be stabilized initially). Ten replicate samples were taken in each plot with a 2.5 cm diameter soil probe and were separated into the organic horizon and the upper mineral soil (0–20 cm). We focused on the organic horizon and upper 20 cm of mineral soil as there are relatively small concentrations of organic matter (and presumably organic P) in deeper soil horizons (Turner et al. 2012b). This yielded three composite samples of the organic horizon and three samples of mineral soil for each dune unit. The soil was air-dried at 30 °C for 10 days and then ground finely in a ball mill.

Phosphorus was extracted by shaking soil (1.50 ± 0.01 g) with 30 mL of a solution containing 0.25 M NaOH and 50 mM Na_2EDTA (sodium ethylenediaminetetraacetate) for 16 h at 22 °C (Bowman and Moir 1993). Each extract was centrifuged at 8,000×*g* for 30 min and the supernatant decanted. A 1 mL aliquot was neutralized using phenolphthalein indicator and 3 M H_2SO_4 and diluted to 20 mL with deionized water for determination of total P by ICP–OES (detection limit 0.008 mg P L^{-1}, equivalent to ~3 mg P kg^{-1}). Reactive P (which approximates inorganic orthophosphate) was determined in the diluted NaOH–EDTA extracts by automated molybdate colorimetry using a Lachat Quikchem 8500 (Hach Ltd, Loveland, CO, USA), with correction for interference from organic matter by analyzing samples without color reagents (detection limit 0.003 mg P L^{-1}, equivalent to ~1 mg P kg^{-1}). Organic (unreactive) P was determined as the difference between total

and reactive P in the extracts. A 20 mL aliquot of each extract was spiked with 1 mL of 50 μg P mL^{-1} methylene diphosphonic acid (MDP) solution as an internal standard, frozen at −35 °C, lyophilized (~48 h), and homogenized by gently crushing to a fine powder.

Solution ^{31}P NMR spectroscopy

For NMR spectroscopy, each lyophilized extract (~100 mg) was re-dissolved in 0.1 mL of deuterium oxide and 0.9 mL of a solution containing 1.0 M NaOH and 100 mM Na_2EDTA, and then transferred to a 5-mm NMR tube. Solution ^{31}P NMR spectra were obtained using a Bruker Avance DRX 500 MHz spectrometer (Bruker, Germany) operating at 202.456 MHz for ^{31}P. Samples were analyzed using a 6 μs pulse (45°), a delay time of 2.0 s, an acquisition time of 0.4 s, and broadband proton decoupling. Approximately 30,000 scans were acquired for each sample. Spectra were plotted with a line broadening of 5 Hz and chemical shifts of signals were determined in parts per million (δ ppm) relative to an external standard of 85% H_3PO_4. Chemical shift is defined by $(V_s - V_R)/V_R \times 10^6$, where V_S and V_R are the frequencies of the sample and reference standard relative to that of the applied magnetic field. Signals were assigned to P compounds based on literature reports of model compounds spiked in NaOH–EDTA soil extracts (Doolette et al. 2009; Turner et al. 2003a). Signal areas were calculated by integration and concentrations of P compounds were calculated from the integral value of the MDP internal standard at $\delta = 17.56 \pm 0.02$ ppm ($n = 10$) for mineral soils and $\delta = 17.38 \pm 0.02$ ppm ($n = 10$) for organic soils. (Note that the MDP signal was set to $\delta = 17.56$ ppm for presentation in figures).

The phosphomonoester region was further studied by spectral deconvolution, to identify the signal areas corresponding to inorganic phosphate and the four IP_6 stereoisomers (*myo*, *scyllo*, *neo*, and D-*chiro*) (Turner et al. 2003b; Turner and Richardson 2004; Turner et al. 2012a). Concentrations of *myo*-IP_6 were determined as the sum of the four signals or by multiplying by six the signal from the C-2 phosphate occurring at approximately $\delta = 6$ ppm. The relationship for *myo*-IP_6 determined by the two procedures was described by the equation: $Y = 0.989x–1.40$; $R^2 = 0.96$; $p < 0.0001$, where x is the concentration of *myo*-IP_6 determined by the sum of signals and Y is the concentration determined from the C-2 phosphate. We used the values determined as the sum of signals in all subsequent calculations. All spectral processing was performed in NMR Utility Transform Software (NUTS) for Windows (Acorn NMR Inc., Livermore, CA, USA).

We did not obtain replicate spectra for each soil, but error for replicate analyses of mineral soils, including extraction and NMR spectroscopy, are approximately 2 % for total organic P, 4 % for phosphate monoesters, and 10 % for DNA (Turner 2008b). It is difficult to estimate a detection limit for organic P compounds using the solution ^{31}P NMR spectroscopy procedure, as this varies among samples depending on parameters such as line broadening and the number of scans obtained, although we consider the approximate detection limit here for an individual signal to be ~1 mg P kg^{-1}. These values are proportionally greater for the inositol hexakisphosphates (e.g., 3 mg P kg^{-1} for D-*chiro*-IP_6) based on the correction factors for the detected signals (see above). All values are expressed on the basis of oven-dry soil weight (105 °C, 24 h).

Results

Phosphorus extraction in NaOH–EDTA

For both organic and mineral soil, P concentrations extracted in NaOH–EDTA tended to increase initially during the early stages of pedogenesis, and then decline to relatively low values in the oldest soils (Table 2). For organic horizons, total P recovery in NaOH–EDTA extracts varied between 64 and 93 % of the total soil P (mean 77.0 ± 3.7 %) (Table 2). In mineral soil, total P recovery in NaOH–EDTA extracts was low for the youngest soil (24 ± 10.6), but accounted for 81–92 % of the total soil P for the remainder of the sequence. The low recovery of total P in the youngest soil reflects the large proportion of the phosphate in primary minerals, which the NaOH–EDTA procedure is not designed to extract (Turner et al. 2005).

The proportions of reactive P (i.e., inorganic orthophosphate) and unreactive P (organic P plus inorganic polyphosphate) in the total extracted P were remarkably similar for organic and mineral soils

Table 2 Concentrations of phosphorus determined in NaOH–EDTA extracts of organic and mineral soil horizons (0–20 cm) along a 6,500 year dune sequence at Haast, New Zealand

Dune stage	Dune age (years B.P.)	Organic horizon			Mineral soil (0–20 cm)		
		Total P (mg P kg^{-1})	Reactive P	Unreactive P	Total P	Reactive P	Unreactive P
1	181	559 ± 85 (63 ± 3)	117 ± 33 (21)	442 ± 53 (79)	72 ± 29 (24 ± 11)	26 ± 6 (37)	46 ± 23 (63)
2	290	581 ± 32 (81 ± 2)	85 ± 11 (15)	495 ± 32 (85)	178 ± 7 (91 ± 1)	26 ± 1 (15)	152 ± 5 (85)
3	392	663 ± 70 (93 ± 3)	125 ± 15 (19)	538 ± 57 (81)	196 ± 9 (85 ± 1)	32 ± 3 (16)	164 ± 9 (84)
4	517	595 ± 17 (91 ± 4)	102 ± 12 (17)	493 ± 10 (83)	178 ± 9 (84 ± 2)	31 ± 3 (18)	147 ± 8 (82)
6	787	538 ± 53 (83 ± 4)	167 ± 43 (31)	371 ± 12 (69)	210 ± 4 (85 ± 2)	34 ± 2 (16)	176 ± 3 (84)
8	1,826	408 ± 12 (66 ± 2)	49 ± 5 (12)	359 ± 12 (88)	126 ± 2 (81 ± 1)	20 ± 1 (16)	106 ± 2 (84)
11	3,384	498 ± 5 (83 ± 1)	74 ± 18 (15)	425 ± 19 (85)	115 ± 2 (81 ± 1)	20 ± 2 (17)	95 ± 4 (83)
12	3,903	312 ± 25 (64 ± 5)	51 ± 9 (16)	261 ± 27 (84)	85 ± 2 (81 ± 1)	10 ± 1 (12)	75 ± 1 (88)
13	4,422	339 ± 11 (69 ± 2)	75 ± 13 (22)	264 ± 15 (78)	97 ± 11 (88 ± 5)	13 ± 1 (13)	85 ± 10 (87)
17	6,500	433 ± 13 (71 ± 1)	45 ± 3 (10)	388 ± 10 (90)	82 ± 5 (81 ± 5)	14 ± <1 (17)	69 ± 5 (83)

Total P was determined in diluted and neutralized extracts by ICP–OES detection, reactive (inorganic) P was determined by molybdate colorimetry (reactive P), and unreactive (organic) P was determined as the difference between total P and reactive P. Values are the mean ± standard error of three replicate samples per dune. Values in parentheses are the proportion (%) of the total soil P extracted in NaOH–EDTA

across the sequence. For both organic and mineral soil across the ten chronosequence stages, reactive P accounted for an average of 18 ± 6 % of the total extracted P, while unreactive P accounted for an average of 82 ± 6 % (Table 2).

Concentrations of total P in NaOH–EDTA extracts of mineral soils determined by NMR spectroscopy corresponded closely with those determined by ICP spectrometry. The relationship was described by the following equation: $Y = 0.998x - 2.127$; $R^2 = 0.994$; where Y = total P determined by solution ^{31}P NMR spectroscopy (i.e., using the internal standard) and x = total P determined by ICP spectrometry. The relationship was less strong for extracts of organic soil, and was described by the equation: $Y = 0.725x + 64.002$; $R^2 = 0.812$. We therefore used total P determined by ICP spectrometry to calculate concentrations of P compounds by solution ^{31}P NMR spectroscopy.

Identification of signals in solution ^{31}P NMR spectroscopy

The NaOH–EDTA extracts contained a variety of inorganic and organic P compounds (Fig. 1). The inorganic phosphates included orthophosphate, pyrophosphate, and long-chain polyphosphate. The organic P compounds included phosphomonoesters, phosphodiesters, phospholipids, and phosphonates.

Of the inorganic phosphates, orthophosphate occurred as a prominent signal at $\delta = 6.17 \pm 0.02$ ppm (mean ± standard deviation of ten spectra) in extracts of organic soil and $\delta = 6.33 \pm 0.02$ ppm in extracts of mineral soil. Pyrophosphate, a polyphosphate with a chain length of two, occurred at $\delta = -4.41 \pm 0.05$ ppm (organic soils) or $\delta = -4.05 \pm 0.05$ ppm (mineral soils). Long-chain polyphosphate, detected at quantifiable concentrations only in extracts of organic soil, gave signals at $\delta = -3.8$ ppm (end-chain phosphates) and between -18 and -21 ppm (mid-chain phosphates). The mean (± standard deviation) chain length calculated from these two signals was 12 ± 3. Of the organic P compounds, phosphomonoesters occurred as a group of signals between $\delta = 3.5$ and 7.0 ppm (excluding the orthophosphate signal), while other prominent signals were assigned to DNA (a broad signal at $\delta = \sim 0$ ppm), phospholipids (small signals between $\delta = 0.5$ and 2.0 ppm), and phosphonate ($\delta = 20.66 \pm 0.01$ ppm).

Within the phosphomonoester pool of mineral soil spectra, we further identified four stereoisomers of inositol hexakisphosphate (Fig. 2). The *myo*

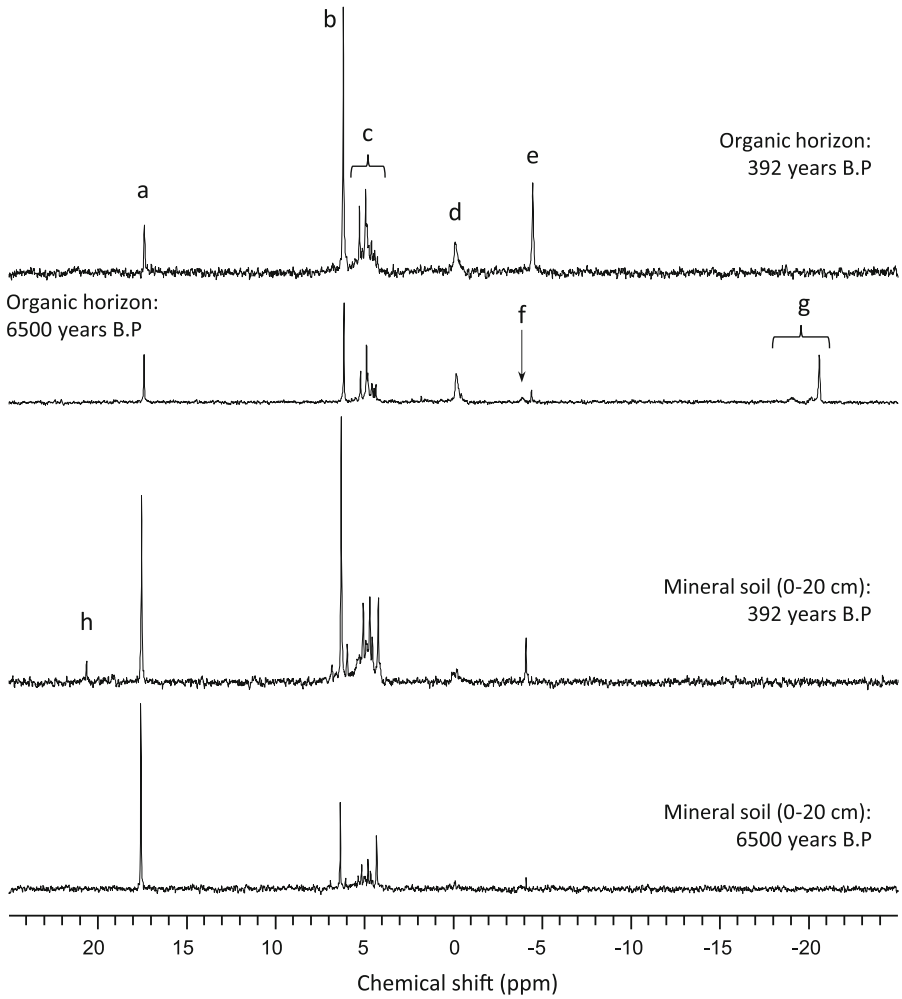

Fig. 1 Solution ^{31}P NMR spectra of NaOH–EDTA extracts of organic and mineral soil from young (392 years before present) and old (6,500 years before present) sites along the Haast soil chronosequence, New Zealand. Signal assignments are as follows: **a** methylene diphosphonic acid (MDP) internal standard; **b** inorganic orthophosphate; **c** phosphomonoesters; **d** DNA; **e** pyrophosphate; **f** end-groups of long-chain inorganic polyphosphate; **g** middle-groups of long-chain inorganic polyphosphate; **h** phosphonate (2-aminoethylphosphonic acid). Spectra are plotted with 5 Hz line broadening and normalized by adjustment of the internal standard to the mean chemical shift for extracts of mineral soil ($\delta = 17.56$ ppm)

stereoisomer was identified as four signals in a 1:2:2:1 ratio at $\delta = 6.01$, 5.10, 4.73, and 4.59 ppm, corresponding to the C2, C1 and C3, C4 and C6, and C5 phosphates, respectively, on the inositol ring (Turner et al. 2003b). The *scyllo* stereoisomer was identified as the prominent signal at $\delta = 4.25 \pm 0.01$ ppm, corresponding to all six phosphates on the inositol ring (Turner and Richardson 2004). The *neo* and D-*chiro* stereoisomers were identified from signals upfield of orthophosphate, with the signal at $\delta = 6.65 \pm 0.02$ ppm assigned to the equatorial phosphate groups of the 2-equatorial/4-axial conformer of D-*chiro*-IP_6, and the signal at $\delta = 6.86 \pm 0.01$ ppm assigned to the equatorial phosphate groups of the 4-equatorial/2-axial conformer of *neo*-IP_6. For quantification, the D-*chiro*-IP_6 and *neo*-IP_6 signals were multiplied by 3.0 and 1.5, respectively (Turner et al. 2012a).

Changes in phosphorus composition during pedogenesis

Organic horizon

Inorganic P in organic soil (Fig. 3a) was dominated by orthophosphate in young soils (i.e., <800 years old), in which it represented between 122 and 199 mg P kg^{-1} (28–40 % of the extracted P) (Table 3). Orthophosphate then declined to <80 mg P kg^{-1} on older soils (15–22 % of the extracted P). Note that orthophosphate concentrations determined by solution ^{31}P NMR spectroscopy were greater than those determined as reactive P by molybdate colorimetry (i.e., compare values in Fig. 3a and Table 2). Such discrepancies occur commonly and might relate to occlusion of orthophosphate within large humic

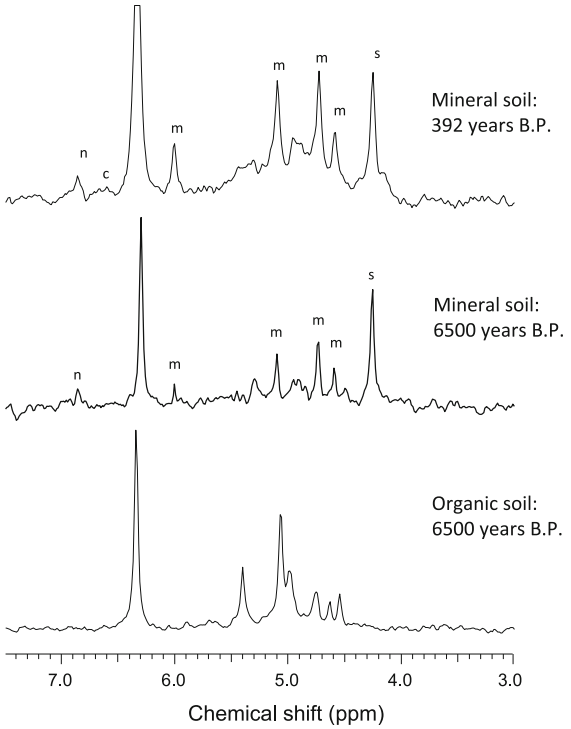

Fig. 2 The phosphomonoester region of solution ^{31}P NMR spectra of NaOH–EDTA extracts of mineral soil from young (392 years before present) and old (6,500 years before present) sites along the Haast soil chronosequence, New Zealand. The mineral soil spectra show signals from the deconvolution procedure, with signal assignments as follows: m, *myo*-inositol hexakisphosphate; s, *scyllo*-inositol hexakisphosphate; n, *neo*-inositol hexakisphosphate; c, D-*chiro*-inositol hexakisphosphate. The same region of an organic horizon extract from the 6,500 year site is shown for comparison, in which signals from the two inositol hexakisphosphate stereoisomers are not present in detectable concentrations

molecules (e.g., Turner et al. 2006). Pyrophosphate followed a similar pattern, increasing initially to 90 mg P kg^{-1} in the first few hundred years of pedogenesis, and then declining to low values ($\leq$14 mg P kg^{-1}) in older soils (Fig. 3a). Pyrophosphate accounted for up to 19 % of the extracted P in young soils (<800 years old), but $\leq$3 % of the extracted P in older soils (Table 3). In contrast to ortho- and pyrophosphate, long-chain polyphosphate was absent from all but one soil during the first 800 years of pedogenesis, but then increased markedly to 46–103 mg P kg^{-1} in older soils (15–25 % of the extracted P) (Fig. 3a, Table 3).

Organic P in organic soil (Fig. 3b) was dominated by phosphomonoesters. Phosphomonoester concentrations were much greater in young soils <800 years old (176–270 mg P kg^{-1}) compared to older soils (80–130 mg P kg^{-1}). Phosphomonoesters also represented a much greater proportion of the extracted P in young soils (40–53 %) than in old soils (29–36 %) (Table 3). Of the phosphodiesters, DNA concentrations (47–85 mg P kg^{-1}) showed no clear pattern across the sequence. However, DNA increased as a proportion of the extracted P, from 9 to 14 % on young soils (<1,000 years) to 19–21 % on older soils. Phospholipids were not detected in soils <800 years old, but represented between 13 and 23 mg P kg^{-1} (4–5 % of extracted P) on older soils. Phosphonates were not detected in any organic soil along the chronosequence.

Mineral soil

Inorganic P in mineral soil (Fig. 3c) was dominated by orthophosphate, with concentrations increasing initially to 52 mg P kg^{-1} after ~800 years of pedogenesis, and then declining to $\leq$25 mg P kg^{-1} on older soils. Orthophosphate accounted for 23–38 % of the extracted P in young mineral soils, declining to 18–20 % on older soils (Table 3). Pyrophosphate followed a similar pattern, increasing initially to ~10 mg P kg^{-1} (4–6 % of the extracted P) in young soils, and then declining to low values (<3 mg P kg^{-1}; <3 % of extracted P) in older soils. Long-chain polyphosphate was detected in only a single sample of mineral soil along the entire chronosequence (a trace was present in the 517 year old soil) (Table 3).

Organic P in mineral soil (Fig. 3d) was dominated by phosphomonoesters, with concentrations increasing initially to 124 mg P kg^{-1} after 800 years of pedogenesis, and then declining to lower values on older soils (56 mg P kg^{-1} after 6,500 years). Phosphomonoesters tended to increase as a proportion of the extracted P as soils aged, from 51 to 66 % on soils <800 years old to 69–75 % on older soils (Table 3). Of the phosphodiesters, DNA concentrations increased to 12 mg P kg^{-1} after ~400 years of pedogenesis, and then declined to <7 ppm on older soils (Fig. 3d). However, DNA varied little as a proportion of the extracted P (4–8 %) along the sequence (Table 3). Phospholipids were detected only in young mineral soils (although not in the youngest soil), where they accounted for ~1 % of extracted P (Table 3). Phosphonates followed a similar pattern, with concentrations up to 5 mg P kg^{-1} in young soils

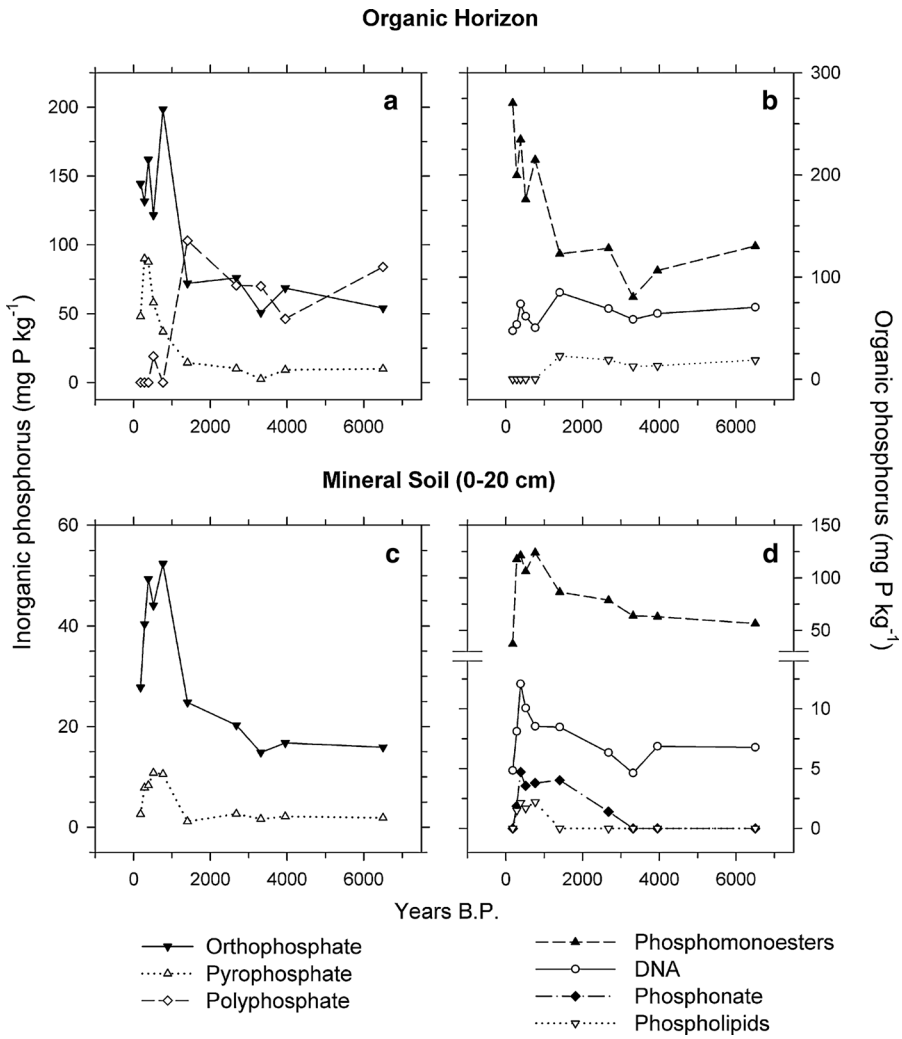

Fig. 3 Concentrations of inorganic and organic phosphorus compounds in the organic horizon and upper mineral soil (0–20 cm) along the Haast chronosequence, New Zealand, determined by NaOH–EDTA extraction and solution ^{31}P NMR spectroscopy

(although not in the youngest soil), declining to undetectable levels in the oldest soils.

Inositol hexakisphosphate stereoisomers

We quantified four stereoisomers of inositol hexakisphosphate in extracts of mineral soils (Table 4). We did not detect quantifiable concentrations of IP_6 in the youngest soil. In the remaining soils, total IP_6 increased to 65.8 mg P kg^{-1} in the early stages of pedogenesis, and then declined to low values in the oldest soils (26.4 mg P kg^{-1} after 6,500 years) (Table 4). Total IP_6 represented between 36.0 and 51.7 % of the total organic P across the chronosequence (mean 44.6 ± 5.2 %) and between 40.2 and 59.1 % of the phosphomonoesters (mean 49.9 ± 6.1 %).

The majority of the IP_6 occurred as the *myo* stereoisomer (i.e., phytic acid); concentrations of *myo*-IP_6 increased to 42.3 mg P kg^{-1} after 392 years, and then declined to 12.7 mg P kg^{-1} in the oldest soil (Fig. 4a). Similarly, *scyllo*-IP_6 increased initially to 16.0 mg P kg^{-1} in the early stages of pedogenesis, and then declined to ~10 mg P kg^{-1} in the oldest soils (Fig. 4a). However, the *myo* stereoisomer declined more rapidly than the *scyllo* stereoisomer, as shown by the increase in the *scyllo* to *myo* ratio through time (Fig. 4b). Indeed, *scyllo*-IP_6 increased continually as a proportion of the soil organic P as soils aged. The *neo* and D-*chiro* stereoisomers were detected in relatively low concentrations; *neo*-IP_6 occurred in concentrations up to 6.5 mg P kg^{-1} and D-*chiro*-IP_6 up to 4.8 mg P kg^{-1} (Table 4). The D-*chiro* isomer occurred in quantifiable concentrations only in intermediate-aged

Table 3 Proportions (%) of phosphorus compounds determined by NaOH–EDTA extraction and solution ^{31}P NMR spectroscopy in the organic horizon and mineral soil (0–20 cm) along a dune sequence at Haast, New Zealand

Dune stage	Dune age (years B.P.)	Inorganic P			Organic P			
		Ortho-phosphate	Pyro-phosphate	Poly-phosphate	Phospho-monoesters	Phosphodiesters		Phosphonate
						DNA	Phospholipids	
		(% of extracted P)						
Organic horizon								
1	181	28.3	9.4	nd	53.0	9.3	nd	nd
2	290	27.7	18.9	nd	42.0	11.3	nd	nd
3	392	29.0	15.7	nd	42.1	13.2	nd	nd
4	517	27.9	13.3	4.4	40.4	14.1	nd	nd
6	787	39.7	7.4	nd	42.9	10.1	nd	nd
8	1826	17.1	3.4	24.6	29.2	20.2	5.4	nd
11	3,384	20.4	2.7	18.9	34.4	18.5	5.1	nd
12	3,903	18.5	0.9	25.4	29.3	21.3	4.6	nd
13	4,422	22.3	3.0	15.0	34.6	20.9	4.3	nd
17	6,500	14.7	2.7	22.8	35.5	19.2	5.1	nd
Mineral soil								
1	181	38.5	3.6	nd	51.3	6.7	nd	nd
2	290	22.7	4.4	nd	66.4	4.6	0.9	1.0
3	392	24.9	4.2	nd	61.3	6.1	1.1	2.4
4	517	25.0	6.1	tr	60.2	5.7	1.0	2.0
6	787	26.0	5.2	nd	61.6	4.2	1.1	1.9
8	1,826	19.9	0.9	nd	69.2	6.8	nd	3.2
11	3,384	18.5	2.4	nd	72.0	5.8	nd	1.3
12	3,903	17.5	1.9	nd	75.1	5.4	nd	nd
13	4,422	18.9	2.4	nd	71.0	7.7	nd	nd
17	6,500	19.6	2.3	nd	69.7	8.4	nd	nd

Values are the proportion (%) of the NaOH–EDTA extractable total phosphorus

nd not detected, *tr* trace

soils, while the *neo* isomer showed no clear pattern along the chronosequence.

Averaged across the nine sites in which IP_6 was quantified (i.e., excluding the youngest soil), *myo*-IP_6 accounted for 54.7 ± 1.8 % of the total IP_6, *scyllo*-IP_6 accounted for 31.3 ± 1.8 %, *neo*-IP_6 accounted for 9.6 ± 0.9 %, and D-*chiro*-IP_6 4.0 ± 1.4 % (Table 4). For the *myo* isomer, the value decreased from 64 % of the total IP_6 after 400 years of pedogenesis to 48 % after 6,500 years (Table 4). In contrast, the *scyllo* isomer increased from 24 % of the total IP_6 after 400 years to 43 % after 6,500 years.

Quantifiable concentrations of IP_6 occurred in the organic soil at only a single site (Dune Unit 5; 782 years B.P.). That sample contained a total IP_6 concentration of 33.5 mg P kg^{-1}, which accounted for 12.6 % of the total organic P. Of this, 80.7 % was *myo*-IP_6 and the remainder was *scyllo*-IP_6. Traces of IP_6 occurred in the organic horizon of some of the younger dunes, but not in dunes >1,000 years old.

Relationship between inositol hexakisphosphate and amorphous metal oxides

In a previous study along the Franz Josef chronosequence, inositol hexakisphosphate (i.e., the sum of *myo*-IP_6 and *scyllo*-IP_6; the *neo* and D-*chiro* isomers had not been identified in ^{31}P NMR spectroscopy at that time) increased during the early stages of pedogenesis and then declined markedly in old soils (Fig. 5a). Two hypotheses were proposed to explain this pattern: the biological utilization of inositol

Table 4 Inositol hexakisphosphate stereoisomers in mineral soil (0–20 cm) determined by NaOH–EDTA extraction, solution ^{31}P NMR spectroscopy, and spectral deconvolution, along a dune sequence at Haast, New Zealand

Dune stage	Dune age (years B.P.)	Total IP_6		(% of total IP_6)			
		(mg P kg^{-1})	% of organic P	*myo*-IP_6	*scyllo*-IP_6	*neo*-IP_6	D-*chiro*-IP_6
1	181	nd	–	nd	nd	nd	nd
2	290	56.7	44.4	61.6	27.4	9.8	tr
3	392	65.8	46.9	64.3	22.2	7.5	5.9
4	517	48.6	40.0	54.1	32.9	7.8	5.2
6	787	49.9	36.0	49.9	31.7	8.8	9.7
8	1,826	51.1	51.6	53.3	28.0	12.7	6.1
11	3,384	40.0	46.3	49.7	32.8	8.4	9.2
12	3,903	29.7	44.4	57.1	34.1	6.4	tr
13	4,422	36.2	51.7	54.0	31.5	14.5	nd
17	6,500	26.4	41.8	48.0	41.3	10.7	nd

Total inositol hexakisphosphate (i.e., the sum of the four stereoisomeric forms) is given as the concentration (mg P kg^{-1}) and proportion (%) of the total organic phosphorus. The four stereoisomers are given as the proportion (%) of the total IP_6

nd not detected, *tr* trace

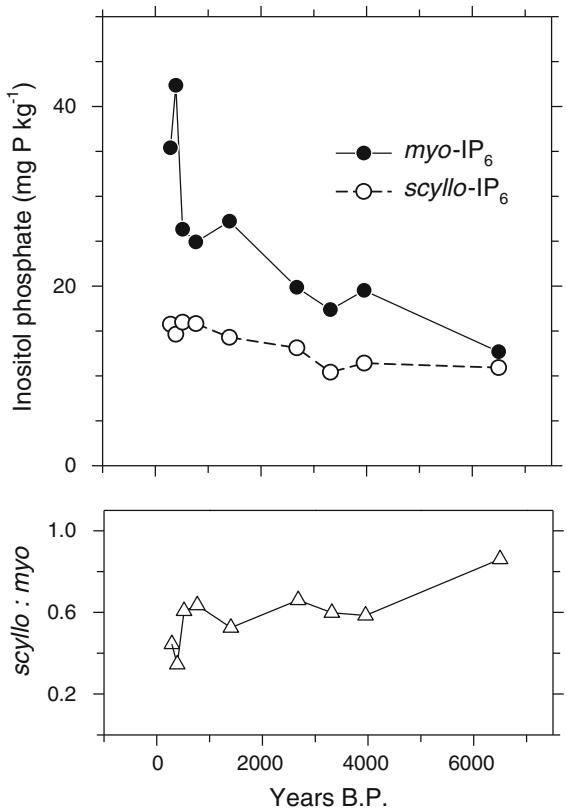

Fig. 4 Concentrations of *myo*- and *scyllo*-inositol hexakisphosphate (*upper panel*) and their ratio (lower panel) in upper mineral soil (0–20 cm) along the Haast chronosequence, New Zealand, determined by NaOH–EDTA extraction, solution ^{31}P NMR spectroscopy, and spectral deconvolution

phosphates under strong biological P stress in older soils, or a decline in the potential for IP_6 stabilization in old soils due to the corresponding decline in amorphous (oxalate-extractable) metal oxides. At Franz Josef, concentrations of amorphous metal oxides closely followed those of IP_6, increasing to >200 mmol kg^{-1} in the early stages of pedogenesis, and then declining strongly as soils aged (Fig. 5a). At Haast, amorphous Al and Fe concentrations increased more or less continuously along the chronosequence (Fig. 5b), and after 6,500 years the combined concentration of ~200 mmol kg^{-1} was similar to the maximum concentration along the Franz Josef chronosequence. Unlike at Franz Josef, however, IP_6 concentrations at Haast did not follow the concentrations of amorphous metals, instead declining from a maximum in ~400 year old soils to low levels in 6,500 year old soils (Fig. 5b).

Discussion

Patterns of phosphorus forms and concentrations along the chronosequence

The Walker and Syers (1976) model of P transformations during pedogenesis predicts a decline in total soil P, the depletion of primary mineral phosphate, and the development of a system dominated by organic P as

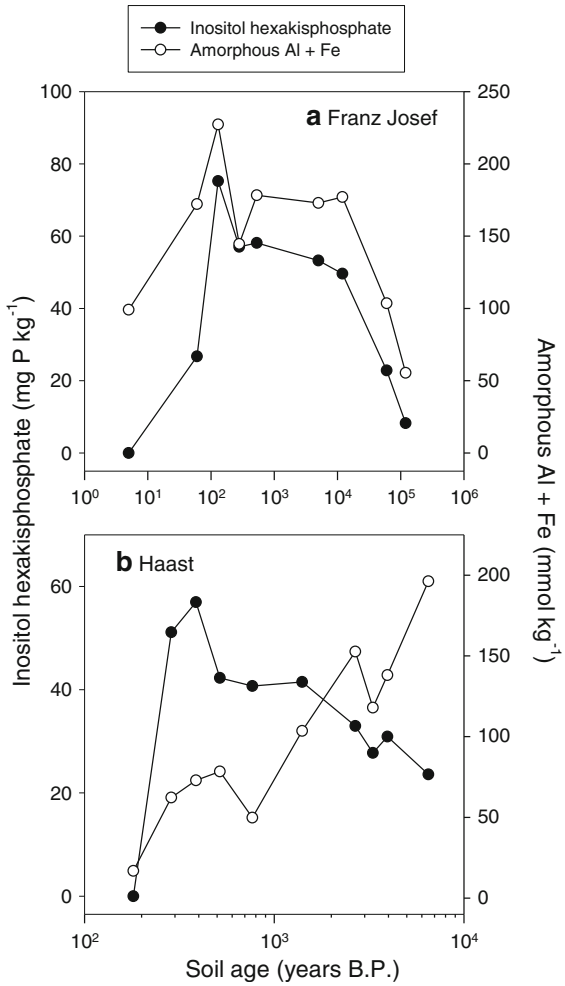

Fig. 5 A comparison of inositol hexakisphosphate (including the *myo* and *scyllo* stereoisomers) and amorphous aluminum and iron extractable in acid-ammonium oxalate, for **a** the Franz Josef post-glacial chronosequence (data from Turner et al. 2007) and **b** the Haast coastal dune chronosequence (current study). Note the different *x* axes, which are on a logarithmic scale, corresponding to 120,000 years of pedogenesis for the Franz Josef system (**a**) and 6,500 years for the Haast system (**b**)

soils age over thousands to millions of years. This pattern has been verified along chronosequences spanning a range of parent material and climate (e.g., Crews et al. 1995; Selmants and Hart 2010; Izquierdo et al. 2013). At Haast, the switch to an organic P dominated system occurs rapidly, with primary mineral phosphate depleted within a few of hundred years of pedogenesis (Turner et al. 2012b). By this stage, soil organic P accounts for more than 80 % of the total soil P and its turnover presumably supplies the majority of the P nutrition of plants and microorganisms. The pace of P transformations at Haast is driven by the warm, wet climate, the relatively low initial total P pool, and the coarse-textured soil. Similar rapid depletion of apatite has been reported for a number of other chronosequences on sandy soils (Syers and Walker 1969; Singleton and Lavkulich 1987; Celi et al. 2013). At the nearby Franz Josef chronosequence, where soils are developed on post glacial deposits and develop into fine-textured soils, the rate of decline in total P is similar to Haast, but total P concentrations remain high for a much longer period of time due to the greater initial P concentration in the schist/greywacke parent material (Walker and Syers 1976; Turner et al. 2012b).

In addition to changes in the overall inorganic and organic P pools along the Haast chronosequence, there are marked changes in the chemical forms of P as pedogenesis proceeds. The concentrations of most compounds, including all organic P compounds in mineral soils, and pyrophosphate and orthophosphate in organic and mineral soils, increased initially in the early stages of pedogenesis and then declined. However, the concentrations of some compounds in the organic horizon increased markedly as soils aged, including long-chain polyphosphate, phospholipids, and DNA. Patterns were similar when compounds were expressed as a proportion of the total extracted P, although the proportion of phosphomonoesters increased in old mineral soils, even though their absolute concentration declined. In addition, some compounds were not detected in old (phospholipids and phosphonates in mineral soil) or young (phospholipids and long-chain polyphosphate in organic soil) soils.

The changes in P composition were particularly marked after 800 years of pedogenesis. This corresponds with major changes in soil morphology and chemistry associated with podzolisation, including a decline in pH, the development of a bleached eluvial horizon, and a pronounced thickening of the organic horizon (Table 1; Turner et al. 2012b). A further major change in the soils after approximately 3,500 years, involving the development of a cemented iron pan and a transformation from Entisols (Spodic Udipsamments) to Spodosols (Typic Placorthods), was not associated with major changes in P pools or chemical composition.

The changes in P compounds during pedogenesis differ in some respects from previous studies, although the organic P composition has been determined along only a handful of chronosequences. Studies of other chronosequences in New Zealand revealed that DNA and pyrophosphate both increased as a proportion of the extracted P as pedogenesis progressed, while IP_6 declined (McDowell et al. 2007; Turner et al. 2007). In contrast, along a 7,800 year marine uplift terrace chronosequence in Sweden, concentrations of pyrophosphate and some phosphomonoesters were greatest in young soils, while DNA, phosphonates, and long-chain polyphosphate were greatest in intermediate aged soils (Vincent et al. 2013).

Inositol hexakisphosphate transformations during ecosystem development

Inositol hexakisphosphate was abundant in mineral soils along the Haast sequence. In agreement with previous studies of chronosequences in New Zealand (McDowell et al. 2007; Turner et al. 2007), IP_6 concentrations were greatest in soils of intermediate fertility and declined to low concentrations in old soils. In addition, there were differences in the patterns of the various stereoisomeric forms along the Haast chronosequence. As reported previously for other chronosequences in New Zealand (McDowell et al. 2007; Turner et al. 2007), *myo*-IP_6 declined more rapidly than *scyllo*-IP_6, as shown by the *scyllo* to *myo* ratio, which presumably reflects the greater resistance of the *scyllo* isomer to enzymatic attack (Cosgrove 1970). In contrast, a study of a 7,800 year marine uplift terrace chronosequence in Sweden reported no clear pattern of IP_6, perhaps because only the organic soil horizon was analyzed and there was little change in total P along the sequence (Vincent et al. 2013).

Signals from *neo* and D-*chiro*-IP_6 have only recently been identified in solution ^{31}P NMR spectroscopy of soil extracts (Turner et al. 2012a), so this is the first study to report the concentrations of all four IP_6 stereoisomers along a soil chronosequence. The D-*chiro* isomer was detected only in intermediate aged soils, while the *neo* isomer showed no clear pattern with ecosystem development. However, the distribution of IP_6 stereoisomers in the soils at Haast is remarkably similar to those reported recently for three soils under temperate grassland from the Falkland Islands (Turner et al. 2012a). In that study, IP_6 accounted for 49 ± 4 % of the total organic P, of which the four isomers constituted 56 % (*myo*-IP_6), 33 % (*scyllo*-IP_6), 6.1 % (*neo*-IP_6), and 5.2 % (D-*chiro*-IP_6) of the total IP_6. At Haast, IP_6 was 45 ± 5 % of the organic P, of which the stereoisomers accounted for 55, 31, 10, and 4 %, respectively, of the total IP_6. The abundance of IP_6 stereoisomers other than *myo*, the only form synthesized by plants, points to the significance of microbial synthesis as a source of IP_6 in these soils (Turner 2007).

The marked decline in inositol phosphates in old, strongly-weathered soils along the Franz Josef chronosequence, on a fine textured soil and over a much longer time scale (Turner et al. 2007), was mirrored by a decline in amorphous Al and Fe oxides, as well as an increase in P limitation. This suggested two possible mechanisms for the decline in inositol phosphates. First, if IP_6 is stabilized by association with amorphous metal oxides (Celi and Barberis 2007), then the decline in Franz Josef soils could be due to a decline in sites for sorption and protection from enzymatic attack. Alternatively, strengthening P limitation as soils age is expected to promote plants (and microbes) that have the capacity to hydrolyze inositol phosphates (e.g., through the synthesis of phytase). This capacity could include mechanisms such as the secretion of organic acids that solubilize IP_6 from binding sites (Giles et al. 2014) or synthesis of the phytase enzyme necessary to dephosphorylate the inositol ring (Hill and Richardson 2007). The first hypothesis—that IP_6 abundance is linked to stabilization potential—is supported by strong relationships between IP_6 and amorphous metal oxides during pedogenesis along the Franz Josef chronosequence (Turner et al. 2007) and in a range of ecosystems (McKercher and Anderson 1968; Turner et al. 2003b; Murphy et al. 2009), as well as the much greater sorption of IP_6 on amorphous compared to crystalline metal oxides (Celi and Barberis 2007). The second hypothesis—that P limitation favors organisms that can access IP_6—is supported by the absence of IP_6 in strongly weathered soils elsewhere, including in lowland tropical rain forests, despite abundant potential for IP_6 stabilization (Vincent et al. 2010; Turner and Engelbrecht 2011).

The results presented here from the Haast sequence indicate that stabilization potential alone is unlikely to account for the decline in IP_6 in old soils, because inositol phosphate concentrations declined at Haast in a similar manner to those at Franz Josef, yet the

concentrations of amorphous metal oxides at Haast increased continually throughout the chronosequence. We therefore conclude that the decline in inositol phosphates at Haast is linked to declining P availability, rather than a change in stabilization potential. It is also possible that inositol phosphate inputs to the soil, either from plant seeds or microbial synthesis, decline as soils age, including through shifts in plant communities (with differences in seed or pollen production) (Turner et al. 2012c) or microbial communities (Jangid et al. 2013). Detailed measurements of IP_6 inputs, stabilization, and hydrolysis are required to resolve this issue.

Contribution of microbial phosphorus to changes in soil phosphorus composition along the chronosequence

It was suggested that much of the non-inositol phosphomonoesters along a marine terrace sequence in Sweden were probably derived from live microbial cells, because approximately 40 % of that pool was identified as RNA degradation products by two dimensional ^{1}H–^{31}P NMR spectroscopy (Vincent et al. 2013). Microbial P constitutes a considerable fraction of the organic P along the Franz Josef chronosequence (Turner et al. 2013) and it is likely that some of the P compounds reported here originate from live microbial cells. This is likely to be relatively small for the mineral soils, however, given the abundance of inositol phosphates, which do not appear to be present in microbial cells (e.g., Bünemann et al. 2008). An important target of future research is to quantify the contribution of microbial P to the soil P pool and the individual compounds along chronosequences from a broad range of environments.

Long-chain polyphosphates were not detected in mineral soils, despite being abundant in the organic horizons of old soils. Polyphosphate can be abundant in some organic soils (e.g., Turner et al. 2004; Vincent et al. 2010) but are rarely so in mineral soils. Polyphosphates are abundant in fungal tissue (Makarov et al. 2005; Bünemann et al. 2008; Koukol et al. 2008) and are eliminated from soil extracts by pretreatment with hexanol (Cheesman et al. 2012), suggesting that the large polyphosphate concentrations in organic horizons at Haast reflect extraction from live fungal tissue. If so, the close relationship between long-chain polyphosphate and phospholipids suggests that both these compounds were extracted from live microbes.

Like polyphosphates, phosphonates also occur in fungal tissue (e.g., Bünemann et al. 2008; Koukol et al. 2008) and are typically detected in cold or acidic soils (Condron et al. 2005), many of which are high in organic matter. However, no phosphonates were detected in the organic horizon along the Haast chronosequence, despite their presence in associated mineral horizons. As phosphonates are presumably synthesized in both organic and mineral soils, this suggests the importance of stabilization on mineral surfaces. Phosphonates declined to undetectable levels in the late stages of the Haast and the Franz Josef chronosequences, suggesting that low P availability is a further factor influencing their presence in soil.

The organisms state factor and phosphorus transformations during ecosystem development

Although soil chronosequences ideally constrain all soil forming factors other than time, the oldest sites have typically experienced marked changes in vegetation and climate (Huggett 1998). Here, the state factor of organisms is relatively well-constrained given that the entire chronosequence is under lowland temperate rainforest drawn from a relatively limited species pool that has been present in the region throughout the Holocene (Li et al. 2008). However, there are changes in the composition of the plant community (Turner et al. 2012c) and microbial community (Jangid et al. 2013) along the chronosequence. Based on a number of lines of evidence, including declining available and total soil P concentrations, widening N:P ratios, and a marked decline in tree basal area on old soils consistent with the concept of forest retrogression (Turner et al. 2012b, c) we interpret the changes in biological communities as being driven primarily by a decline in P availability as soils age over 6,500 years of pedogenesis. These changes in turn are likely to influence the soil organic P composition as soils age, for example if P stress promotes organisms that can acquire P from more recalcitrant forms of soil organic P (see above). As a result, although variation in soil P composition along the chronosequence are driven in large part by changes in the physical and chemical properties of the soils during pedogenesis, at least some of the changes in

soil organic P composition are a response to, as well as a a driver of, changes in biological communities.

Ecological significance of changes in soil phosphorus composition during pedogenesis

The variation in P composition between mineral and organic soils and during pedogenic time has potential ecological significance, because it was previously reported that changes in the species composition of the seedling community were related strongly to nutrient availability in the organic horizon, whereas changes in the adult tree community was associated with nutrient availability in the mineral soil (Turner et al. 2012c). This presumably reflects differences in rooting depth between seedlings and mature trees, and raises the possibility that changes in the P composition of the organic horizon influence the seedling community by altering the availability of organic and inorganic forms of P. Long-term changes in P composition might also influence the competitive ability of adult tree species during ecosystem development, which shift from dominance by the conifer *D. cupressinum* on young soils, to a mixed conifer–broadleaf community on older soils (Turner et al. 2012c). One species, *N. menziesii*, appears as saplings and adult trees only on the oldest dunes and is the only ectomycorrhizal tree that occurs along the sequence. As the enzymatic functions of ectomycorrhizal fungi allow them to access organic P and nitrogen compounds directly from the soil (Read and Perez-Moreno 2003), this presumably provides an important advantage to *N. menziesii* growing on the most infertile soils.

Acknowledgments We thank Amanda Black, Andre Eger, and Victoria Nall, and (Lincoln University) for field assistance and Alex Blumenfeld (University of Idaho) and Dayana Agudo (STRI) for laboratory support. Funding for travel and consumables was provided by Lincoln University.

References

Bowman RA, Cole CV (1978) Transformations of organic phosphorus substrates in soils as evaluated by $NaHCO_3$ extraction. Soil Sci 125:49–54

Bowman RA, Moir JO (1993) Basic EDTA as an extractant for soil organic phosphorus. Soil Sci Soc Am J 57:1516–1518

Bünemann EK, Smernik RJ, Doolette AL, Marschner P, Stonor R, Wakelin SA, McNeill AM (2008) Forms of phosphorus in bacteria and fungi isolated from two Australian soils. Soil Biol Biochem 40:1908–1915

Celi L, Barberis E (2007) Abiotic reactions of inositol phosphates in soil. In: Turner BL, Richardson AE, Mullaney EJ (eds) Inositol phosphates: linking agriculture and the environment. CAB International, Wallingford, pp 207–220

Celi L, Cerli C, Turner BL, Santoni S, Bonifacio E (2013) Biogeochemical cycling of soil phosphorus during natural revegetation of *Pinus sylvestris* on disused sand quarries in Northwestern Russia. Plant Soil 367:121–134

Chadwick OA, Chorover J (2001) The chemistry of pedogenic thresholds. Geoderma 100:321–353

Cheesman AW, Turner BL, Reddy KR (2012) Soil phosphorus forms along a strong nutrient gradient in a tropical ombrotrophic wetland. Soil Sci Soc Am J 76:1496–1506

Condron LM, Turner BL, Cade-Menun BJ (2005) The chemistry and dynamics of soil organic phosphorus. In: Sims JT, Sharpley AN (eds) Phosphorus: agriculture and the environment. ASA-CSSA-SSSA, Madison, pp 87–121

Cosgrove DJ (1970) Inositol phosphate phosphatases of microbiological origin. Inositol phosphate intermediates in the dephosphorylation of the hexaphosphates of *myo*-inositol, *scyllo*-inositol, and D-*chiro*-inositol by a bacterial (*Pseudomonas* sp.) phytase. Aust J Biol Sci 23:1207–1220

Crews TE, Kitayama K, Fownes JH, Riley RH, Herbert DA, Mueller-Dombois D, Vitousek PM (1995) Changes in soil phosphorus fractions and ecosystem dynamics across a long chronosequence in Hawaii. Ecology 76:1407–1424

Doolette AL, Smernik RJ, Dougherty WJ (2009) Spiking improved solution phosphorus-31 nuclear magnetic resonance identification of soil phosphorus compounds. Soil Sci Soc Am J 73:919–927

Eger A, Almond P, Wells A, Condron LM (2013) Quantifying ecosystem rejuvenation: foliar nutrient concentrations and vegetation communities across a dust gradient and a chronosequence. Plant Soil 367:93–109

Giles CD, Hsu P-C, Richardson AE, Hurst MRH, Hill JE (2014) Plant assimilation of phosphorus from an insoluble organic form is improved by addition of an organic anion producing *Pseudomonas* sp. Soil Biol Biochem 68:263–269

Hill JE, Richardson AE (2007) Isolation and assessment of microorganisms that utilize phytate. In: Turner BL, Richardson AE, Mullaney EJ (eds) Inositol phosphates: linking agriculture and the environment. CAB International, Wallingford, pp 61–77

Huggett RJ (1998) Soil chronosequences, soil development, and soil evolution: a critical review. Catena 32:155–172

Izquierdo JE, Houlton BZ, van Huysen TL (2013) Evidence for progressive phosphorus limitation over long-term ecosystem development: examination of a biogeochemical paradigm. Plant Soil 367:135–147

Jangid K, Whitman WB, Condron LM, Turner BL, Williams ME (2013) Bacterial community composition during pedogenesis along a coastal dune system under lowland temperate rainforest in New Zealand. Plant Soil 367:235–247

Koukol O, Novák F, Hrabal R (2008) Composition of the organic phosphorus fraction in basidiocarps of saprotrophic and mycorrhizal fungi. Soil Biol Biochem 40:2464–2467

Li X, Rapson GL, Flenley JR (2008) Holocene vegetational and climatic history, Sponge Swamp, Haast, south-western New Zealand. Quat Int 184:129–138

Loeppert RH, Inskeep WP (1996) Iron. In: Sparks DL et al (eds) Methods of Soil Analysis, Part 3 – Chemical Methods. Soil Science Society of America, Madison, pp 639–664

Makarov MI, Haumaier L, Zech W, Marfenina OE, Lysak LV (2005) Can ^{31}P NMR spectroscopy be used to indicate the origins of soil organic phosphates? Soil Biol Biochem 37:15–25

McDowell RW, Cade-Menun B, Stewart I (2007) Organic phosphorus speciation and pedogenesis: analysis by solution ^{31}P nuclear magnetic resonance spectroscopy. Eur J Soil Sci 58:1348–1357

McKercher RB, Anderson G (1968) Content of inositol penta- and hexaphosphates in some Canadian soils. J Soil Sci 19:47–55

Murphy PNC, Bell A, Turner BL (2009) Phosphorus speciation in temperate basaltic grassland soils by solution ^{31}P NMR spectroscopy. Eur J Soil Sci 60:638–651

Palmer RWP, Doyle RB, Grealish GJ, Almond PC (1986) Soil studies in south Westland, 1984/1985. Soil Bureau District Office Report NP 2. Department of Scientific and Industrial Research, New Zealand.

Peltzer DA, Wardle DA, Allison VJ, Baisden WT, Bardgett RD, Chadwick OA, Condron LM, Parfitt RL, Porder S, Richardson SJ, Turner BL, Vitousek PM, Walker J, Walker LR (2010) Understanding ecosystem retrogression. Ecol Monogr 80:509–529

Read DJ, Perez-Moreno J (2003) Mycorrhizas and nutrient cycling in ecosystems—a journey towards relevance? New Phytol 157:475–492

Saunders WMH, Williams EG (1955) Observations on the determination of total organic phosphorus in soils. J Soil Sci 6:254–267

Selmants PC, Hart SC (2010) Phosphorus and soil development: does the Walker and Syers model apply to semiarid ecosystems? Ecology 91:474–484

Singleton GA, Lavkulich LM (1987) Phosphorus transformations in a soil chronosequence, Vancouver Island, British Columbia. Can J Soil Sci 67:787–793

Syers JK, Walker TW (1969) Phosphorus transformations in a chronosequence of soils developed on wind-blown sand in New Zealand I. Total and organic phosphorus. J Soil Sci 20:57–64

Turner BL (2007) Inositol phosphates in soil: amounts, forms and significance of the phosphorlyated inositol stereoisomers. In: Turner BL, Richardson AE, Mullaney EJ (eds) Inositol phosphates: linking agriculture and the environment. CAB International, Wallingford, pp 186–207

Turner BL (2008a) Resource partitioning for soil phosphorus: a hypothesis. J Ecol 96:698–702

Turner BL (2008b) Soil organic phosphorus in tropical forests: an assessment of the NaOH–EDTA extraction procedure for quantitative analysis by solution ^{31}P NMR spectroscopy. Eur J Soil Sci 59:453–466

Turner BL, Engelbrecht BMJ (2011) Soil organic phosphorus in lowland tropical rain forests. Biogeochemistry 103:297–315

Turner BL, Richardson AE (2004) Identification of *scyllo*-inositol phosphates in soils by solution phosphorus-31 nuclear magnetic resonance spectroscopy. Soil Sci Soc Am J 68:802–808

Turner BL, Mahieu N, Condron LM (2003a) Phosphorus-31 nuclear magnetic resonance spectral assignments of phosphorus compounds in soil NaOH–EDTA extracts. Soil Sci Soc Am J 67:497–510

Turner BL, Mahieu N, Condron LM (2003b) Quantification of *myo*-inositol hexakisphosphate in alkaline soil extracts by solution ^{31}P NMR spectroscopy and spectral deconvolution. Soil Sci 168:469–478

Turner BL, Baxter R, Mahieu N, Sjögersten S, Whitton BA (2004) Phosphorus compounds in subarctic Fennoscandian soils at the mountain birch (*Betula pubescens*)–tundra ecotone. Soil Biol Biochem 36:815–823

Turner BL, Cade-Menun BJ, Condron LM, Newman S (2005) Extraction of soil organic phosphorus. Talanta 66:294–306

Turner BL, Newman S, Reddy KR (2006) Overestimation of organic phosphorus in wetland soils by alkaline extraction and molybdate colorimetry. Environ Sci Technol 40:3349–3354

Turner BL, Condron LM, Richardson SJ, Peltzer DA, Allison VJ (2007) Soil organic phosphorus transformations during pedogenesis. Ecosystems 10:1166–1181

Turner BL, Cheesman AW, Godage HY, Riley AM, Potter BVL (2012a) Determination of *neo*- and D-*chiro*-inositol hexakisphosphate in soils by solution ^{31}P NMR spectroscopy. Environ Sci Technol 46:4994–5002

Turner BL, Condron LM, Wells A, Andersen KM (2012b) Soil nutrient dynamics during podzol development under lowland temperate rain forest. Catena 97:50–62

Turner BL, Wells A, Andersen KM, Condron LM (2012c) Patterns of tree community composition along a coastal dune chronosequence in lowland temperate rain forest in New Zealand. Plant Ecol 213:1525–1541

Turner BL, Lambers H, Condron LM, Cramer MD, Leake JR, Richardson AE, Smith SE (2013) Soil microbial biomass and the fate of phosphorus during long-term ecosystem development. Plant Soil 367:225–234

Vincent AG, Turner BL, Tanner EVJ (2010) Soil organic phosphorus dynamics following perturbation of litter cycling in a tropical moist forest. Eur J Soil Sci 61:48–57

Vincent AG, Vestergren J, Gröbner G, Persson P, Schleucher J, Giesler R (2013) Soil organic phosphorus transformations in a boreal forest chronosequence. Plant Soil 367:149–162

Vitousek PM (2004) Nutrient cycling and limitation. Princeton University Press, Princeton

Walker TW, Syers JK (1976) The fate of phosphorus during pedogenesis. Geoderma 15:1–19

Wells A, Goff J (2006) Coastal dune ridge systems as chronological markers of palaeoseismic activity: a 650-year record from southwest New Zealand. Holocene 16:543–550

Wells A, Goff J (2007) Coastal dunes in Westland, New Zealand, provide a record of paleoseismic activity on the Alpine fault. Geology 35:731–734